Simulations of Ellipsoidal PBH formation and non-spherical effects on the PBH mass function

Albert Escrivà
postdoc at NAOJ (Tokyo), before in Nagoya University

Focus week on PBHs. IPMU 2024

Based on:

A. Escrivà and C.M Yoo. Arxiv: 2410.03451
A. Escrivà and C.M Yoo. Arxiv: 2410.03452

Introduction and motivation

There are several scenarios and mechanisms for PBH formation

But, let's focus on the scenario of PBH formation from the collapse of super-horizon curvature fluctuations generated during inflation

⇓

Sufficiently large fluctuations generated during inflation (very rare events) will collapse forming PBHs during the radiation epoch after they reenter the cosmological horizon.

In general, we assume spherical symmetry in numerical simulations + statistical estimation of the PBH abundance

But actually, why?...

Introduction and motivation

Astrophys.J. 304 (1986) 15-61

According to BBKS (peak theory), you need large peaks to produce a large fraction of PBHs in the form of dark matter (without over-producing)

Consider, for instance, a monochromatic PS

$$\mathcal{P}_\zeta = \mathcal{A}_\zeta \delta(\ln(k/k_p))$$

$$\mathcal{A}_\zeta = \sigma_0^2$$

$$\zeta_{\rm sp} = \mu \, {\rm sinc}(k_p r)$$

(curvature fluctuation)

(Assume spherical symmetry)

$$\nu = \frac{\mu}{\sigma_0}$$

height of the peak

(perfect fluid)

$$P = w\rho$$

$$f_{\rm PBH}(M) = \frac{M\, n_{\rm PBH}(M)}{3M_{\rm pl}^2 H_0^2 \Omega_{\rm DM}}$$

$$n_{\rm pk}(\nu) = \frac{1}{(2\pi)^2}\frac{1}{3^{3/2}} k_p^3 f(\nu) \frac{1}{\sqrt{\mathcal{A}_\zeta}} e^{-\frac{1}{2}\nu^2}$$

C.M. Yoo, T. Harada, J. Garriga, K. Kohri. Arxiv: 1805.03946

Typical amplitude

μ_t

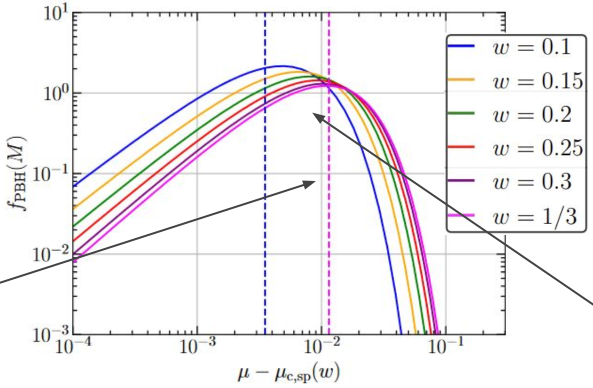

Fluctuations very close to its threshold

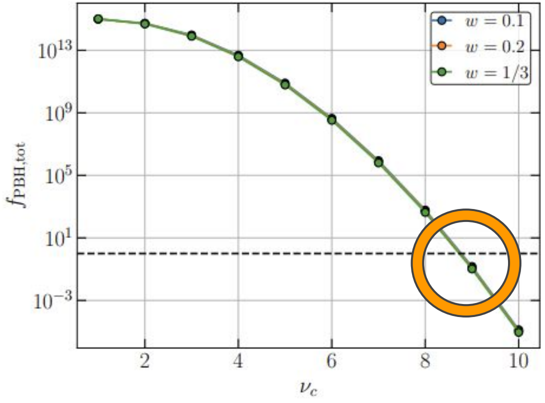

Introduction and motivation

ellipsoids

sphere

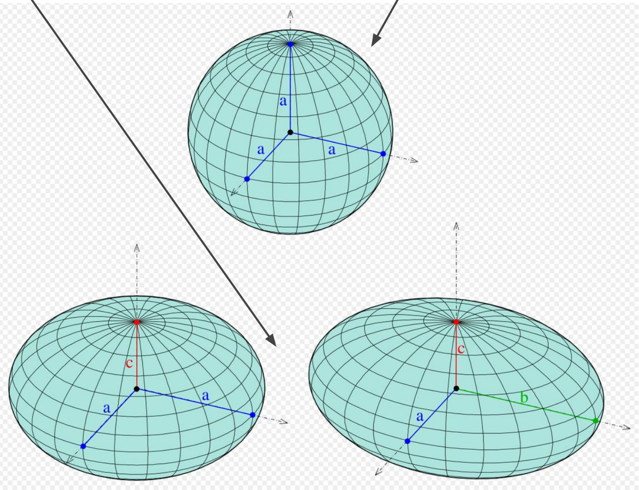

Source: wikipedia

Peak theory tell us how likely are non-spherical configurations

Non-spherical configurations are characterized by an "ellipticity" (e) and "prolatenes" (p)

$$\zeta(\vec{r}) \approx \zeta(\vec{r}=0) - \sum_l \lambda_l \frac{r_l^2}{2} \quad \text{where } \lambda_l \text{ are the eigenvalues of } -\partial_i \partial_j \zeta$$

$$e = \frac{\lambda_1 - \lambda_3}{2\sum_i \lambda_i}, \qquad p = \frac{\lambda_1 - 2\lambda_2 + \lambda_3}{2\sum_i \lambda_i}$$

$$\lambda_1 = \frac{\xi \sigma_2}{3}(1 + 3e + p),$$
$$\lambda_2 = \frac{\xi \sigma_2}{3}(1 - 2p),$$
$$\lambda_3 = \frac{\xi \sigma_2}{3}(1 - 3e + p).$$

$$\xi \equiv -\nabla^2 \zeta\big|_{\vec{r}=0} / \sigma_2$$

$$\zeta(r) \approx \zeta(\vec{r}=0) - \frac{\xi\, \sigma_2}{3} \frac{r^2}{2} \left[1 + A(e,p)\right],$$

Non-spherical contribution

$$A(e,p) = 3e\left[1 - \sin^2\theta(1 + \sin^2\phi)\right] + p\left[1 - 3\sin^2\theta \cos^2\phi\right]$$

Introduction and motivation

(e) and (p) follows a specific probability distribution

$$\mathcal{P}_{\rm e,p}(e,p\,|\,\nu,\xi) = \frac{3^2 5^{5/2}}{\sqrt{2\pi}}\frac{\xi^8}{f(\xi)}\exp\left\{-\frac{5}{2}\xi^2(3e^2+p^2)\right\}W(e,p),$$

$$W(e,p) = (1-2p)\left[(1+p)^2-(3e)^2\right]e(e^2-p^2)\chi(e,p),$$

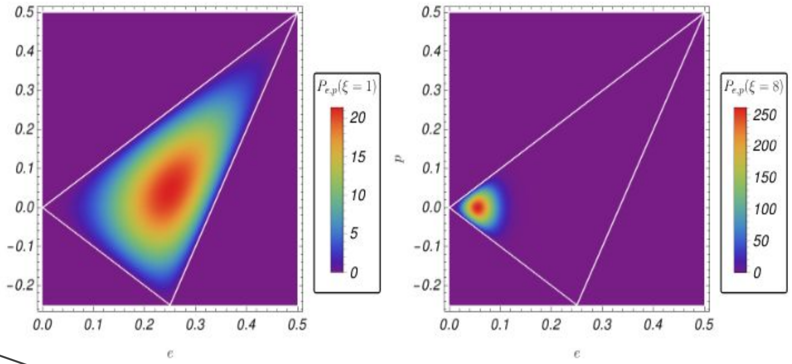

The deviation from sphericity for large peaks is "small"

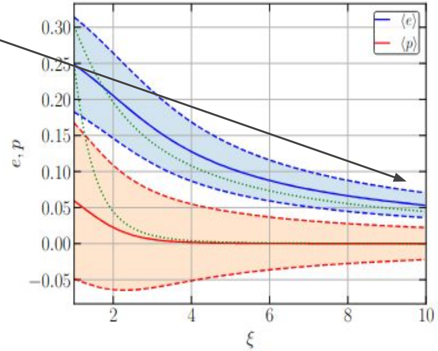

But, nothing tell us that we can directly assume spherical symmetry as a good approximation. **We need to test with simulations!**

Some questions we want to adress

- Deviations from sphericity following peak theory (most likely configurations) make the collapse easier or harder, how much? How is the threshold affected by non-sphericities and including the dependence on the amplitude of the fluctuation?
- The assumption of spherical symmetry is reliable? How is mass function affected by non-sphericities?
- What differences may we observe (regarding the impact of non-spherical effects) when comparing radiation with soft-equation of state?
- What is the effect of non-sphericities on the dynamics of PBH formation for the most likely initial configurations?
- What is the dependence of the threshold on the non-spherical parameters (e,p)?

Numerical method and procedure

We need to perform 3+1 relativistic numerical simulations:
we use BSSN formalism with **COSMOS code** (*Yoo san talk yesterday*)

H. Okawa, H. Witek and V. Cardoso. Arxiv: 1401.1548
C.M. Yoo and H. Okawa. Arxiv: 1404.1435
Similar settings to:
C.M. Yoo, T. Harada, H. Okawa. Arxiv: 2004.01042
C. M. Yoo. Arxiv: 2403.11147

$$ds^2 = -\alpha^2 dt^2 + \tilde{\psi}^4 \tilde{\gamma}_{ij}(dx^i + \beta^i dt)(dx^j + \beta^j dt),$$

$$T_{\mu\nu} = (\rho + P) u_\mu u_\nu + P g_{\mu\nu},$$

(perfect fluid)

We also use spherical code (SPriBosH) to compute the spherical threshold efficiently, which helps us set up the convenient grid (number of points) in the COSMOS code. A.Escrivà. arXiv:1907.13065

The initial conditions are fixed by the curvature fluctuation at super-horizon scales

$$\tilde{\psi} = a^{1/2}\Psi = a^{1/2}\exp(-\zeta/2)$$

The evolution equations in a cosmological setting are given in

T. Harada, C.-M. Yoo, T. Nakama and Y. Koga. Arxiv:1503.03934.

Introduction and motivation

ellipsoids

Peak theory tell us how likely are non-spherical configurations

Non-spherical configurations are characterized by an “ellipticity” (e) and “prolatenes” (p)

$$\zeta(\vec{r}) \approx \zeta(\vec{r}=0) - \sum_l \lambda_l \frac{r_l^2}{2} \quad \text{where } \lambda_l \text{ are the eigenvalues of } -\partial_i\partial_j\zeta$$

$$e = \frac{\lambda_1 - \lambda_3}{2\sum_i \lambda_i}, \qquad p = \frac{\lambda_1 - 2\lambda_2 + \lambda_3}{2\sum_i \lambda_i}$$

$$\lambda_1 = \frac{\xi\sigma_2}{3}(1+3e+p),$$
$$\lambda_2 = \frac{\xi\sigma_2}{3}(1-2p),$$
$$\lambda_3 = \frac{\xi\sigma_2}{3}(1-3e+p).$$

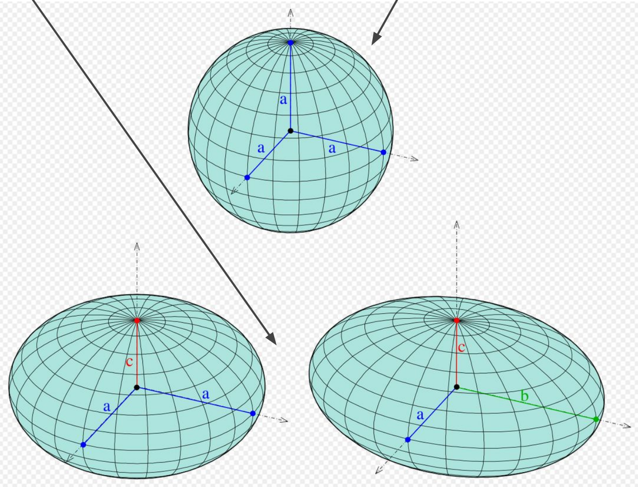

Source: wikipedia

$$\xi \equiv -\nabla^2\zeta\big|_{\vec{r}=0}/\sigma_2$$

$$\zeta(r) \approx \zeta(\vec{r}=0) - \frac{\xi\,\sigma_2}{3}\frac{r^2}{2}\left[1 + A(e,p)\right],$$

Non-spherical contribution

$$A(e,p) = 3e\left[1 - \sin^2\theta(1+\sin^2\phi)\right] + p\left[1 - 3\sin^2\theta\cos^2\phi\right]$$

Initial non-spherical curvature profile

Typical profile following peak theory:

$$\frac{\bar{\zeta}}{\sigma_0} = \frac{\nu}{1-\gamma^2}\left(\psi + R_s^2\frac{\nabla^2\psi}{3}\right) - \frac{\xi/\gamma}{(1-\gamma^2)}\left(\gamma^2\psi + \frac{R_s^2\nabla^2\psi}{3}\right) + \frac{5}{2}R_s^2\left(\frac{\xi}{\gamma}\right)\left(\frac{\psi'}{r} - \frac{\nabla^2\psi}{3}\right)A(e,p)$$

For the monochromatic case:

$\psi(r) = \mathrm{sinc}(k_p r)$ with $\gamma = 1$ and $R_s = \sqrt{3}/k_p$ since $\sigma_n = \sigma_0 k_p^n$.

$$\bar{\zeta} = \zeta_{\rm sp} + \mu\frac{5A(e,p)}{2k_p^3 r^3}\left(3k_p r\cos(k_p r) + (r^2k_p^2 - 3)\sin(k_p r)\right)$$

$$A(e,p) = \frac{3e}{r^2}(z^2 - y^2) + p\left[1 - 3\left(\frac{x}{r}\right)^2\right]$$

$$\zeta_{\rm sp} = \mu\,\mathrm{sinc}(k_p r)$$

(Initial condition of the curvature fluctuation)

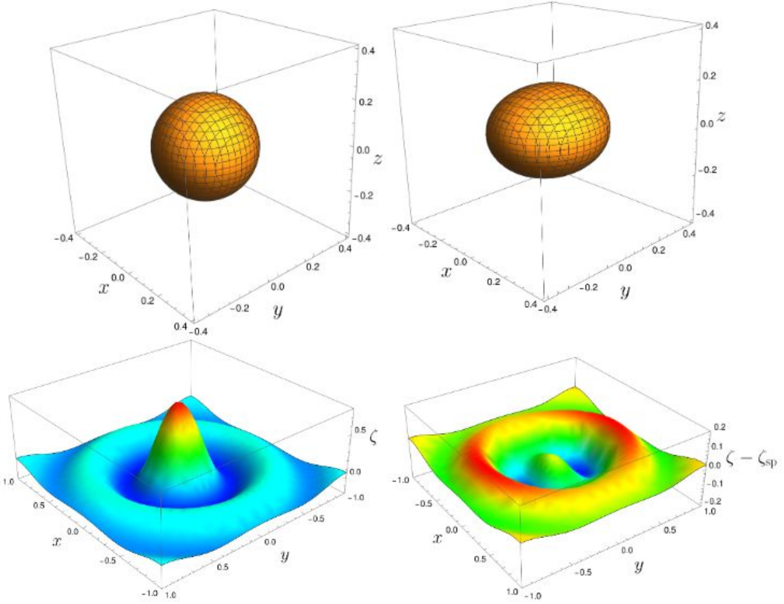

Dynamics of the gravitational collapse

We take a typical amplitude, above the threshold $\mu_t > \mu_c(e,p)$

We observe a damping oscillatory behaviour of the ellipticity.

Example of the collapse for e=0.08, p=0.0 with w=1/3

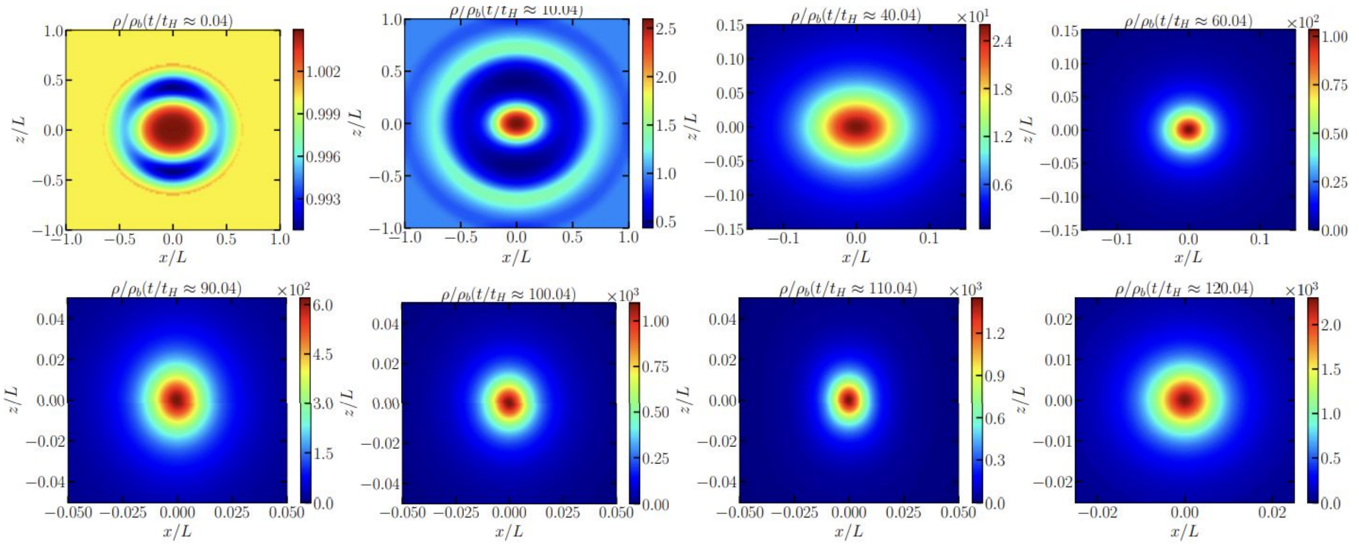

At very late times, the shape is almost spherical

non-spherical effects tend to slow down the collapse and can significantly increase the collapse time

Consistent with non-spherical simulations of collapse of perfect fluid in asymptotically flat spacetime (with "small" deviations from sphericity)

J. Celestino, T.W. Baumgarte. Arxiv: 1805.10442
T.W. Baumgarte, P.J. Montero. Arxiv:1509.08730

Dynamics of the gravitational collapse

$$U^\mu = u^\mu/\Gamma - n^\mu$$

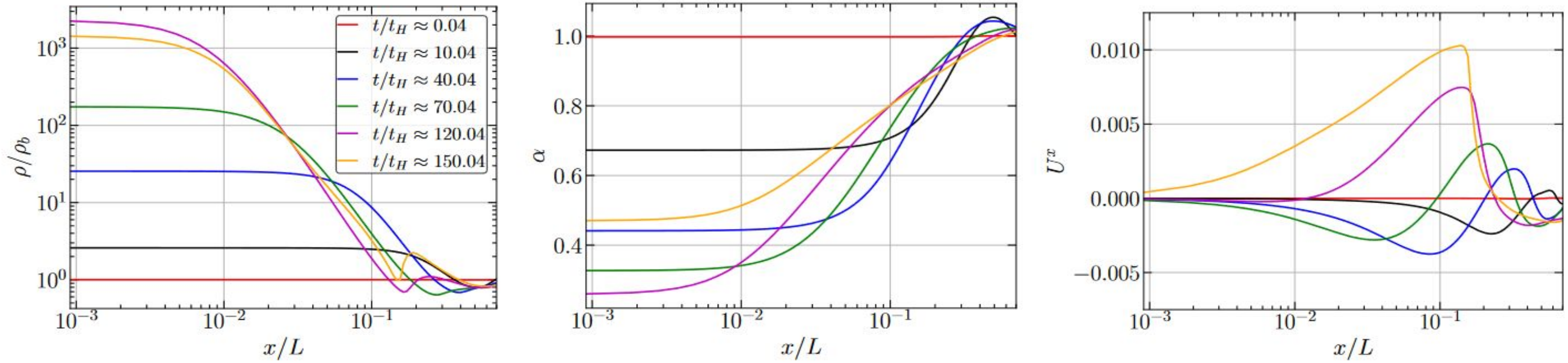

We use the lapse function at the origin to infer the formation of an apparent horizon or not.

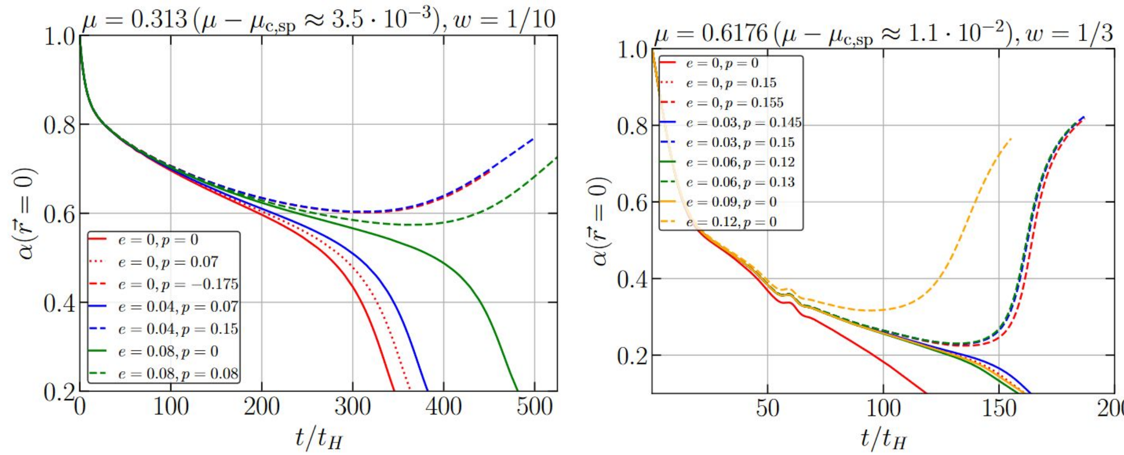

Non-spherical thresholds (e,p) for fixed amplitude

Doing several iterations with a bisection method we can obtain the critical configuration (ec,pc)

We find that the thresholds are well described by a *superellipse* curve for fixed $\mu = \mu_t$

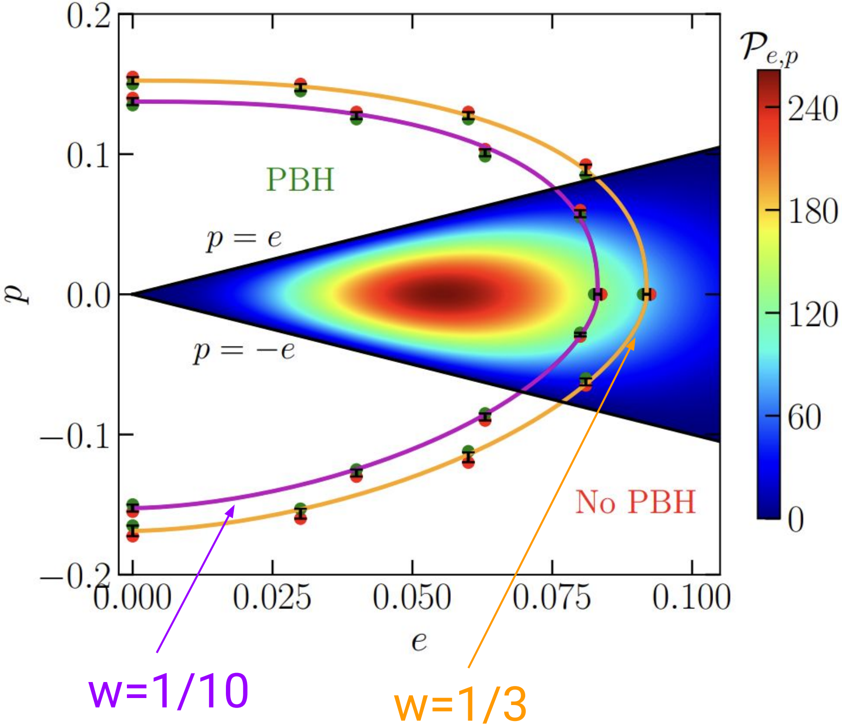

$$\left(\frac{\tilde{p}_c^{\pm}(e)}{p_0^{\pm}}\right)^{n^{\pm}} + \left(\frac{e}{e_0}\right)^{n^{\pm}} = 1 \Rightarrow \tilde{p}_c^{\pm}(e) = \pm p_0^{\pm}\left[1 - \left(\frac{e}{e_0}\right)^{n^{\pm}}\right]^{1/n^{\pm}}$$

universality?

$$n^{+} \approx 2.44 \pm 0.03\,,\; n^{-} \approx 1.70 \pm 0.02 \;(w = 1/3)$$

$$n^{-} \approx 2.53 \pm 0.10\,,\; n^{-} \approx 1.70 \pm 0.05 \;(w = 1/10)$$

We may conjecture for other amplitudes that:

$$\tilde{p}_0^{\pm}(\mu) = \tilde{p}_0^{\pm}(\mu_t) \times \tilde{e}_c(\mu)/\tilde{e}_c(\mu_t)$$

Critical ellipticity as a function of the initial amplitude

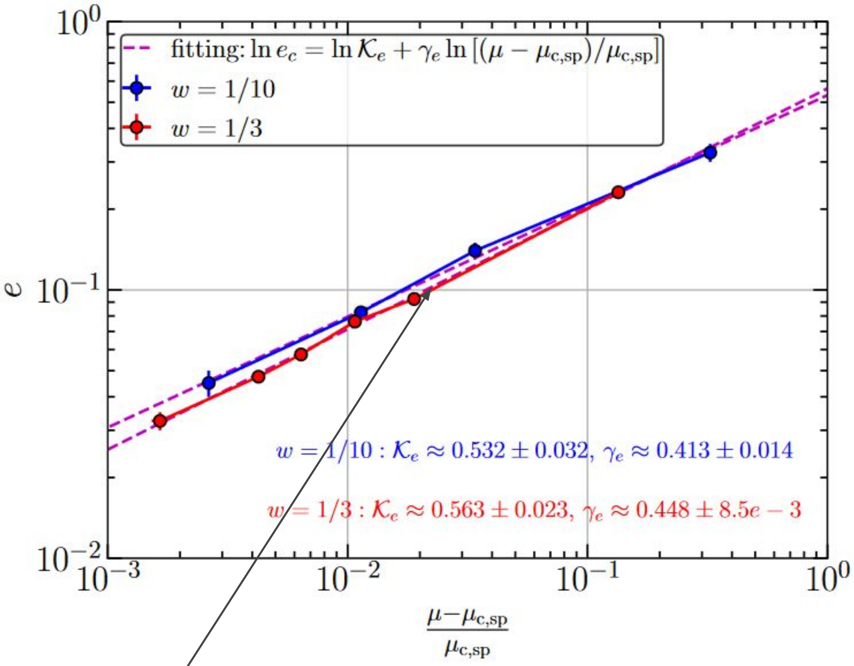

We fix p=0, then let's focus on the ellipticity (e) in terms of the amplitude of the curvature fluctuation

We find that our results closely follow a power law relation

$$\tilde{e}_c(\mu) = \mathcal{K}_e \left(\frac{\mu - \mu_{c,sp}}{\mu_{c,sp}} \right)^{\gamma_e}$$

Interestingly, we don't find significant differences between both w's

We may expect only significant difference for the case of dust

Non-spherical effects make the collapse harder, in comparison with the spherical case

Impact of non-sphericities on the production rate?

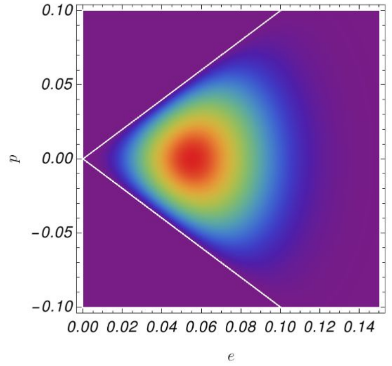

We define for simplicity this domain of integration:

$$\mathcal{R}(\mu) \in \{0 \leq e \leq \tilde{e}_c(\mu)\,,\, -\tilde{e}_c(\mu) \leq p \leq \tilde{e}_c(\mu)\}$$

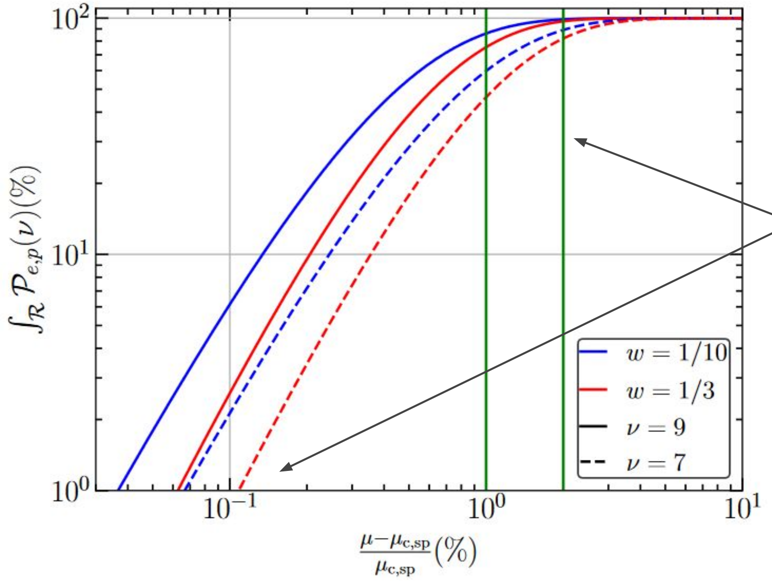

<u>Non-spherical effects are very significant in the critical regime</u>, preventing a large fraction of configurations from collapsing into black holes

A shift of 1-2 % in the threshold (compared with spherical case) makes ~90% of the configurations to collapse

Consistent with the results of a Gaussian profile
C.M. Yoo, T. Harada, H. Okawa. Arxiv: 2004.01042

What is the consequence of that for the PBH mass function?

PBH mass function including non-spherical effects

Let's move to the mass function estimation

Please check the BBKS paper for more details

peak number density distribution

$$\mathcal{N}_{\rm pk}(\nu,\xi,e,p)\,{\rm d}\nu\,{\rm d}\xi\,{\rm d}e\,{\rm d}p =$$

$$= \frac{5^{5/2}3^{1/2}}{(2\pi)^3}\left(\frac{\sigma_2}{\sigma_1}\right)^3 \frac{\exp\{-\bar{Q}\}}{\sqrt{1-\gamma^2}}\xi^6 W(e,p)\,{\rm d}\nu\,{\rm d}\xi\,{\rm d}e\,{\rm d}p$$

$$W(e,p) = (1-2p)\left[(1+p)^2-(3e)^2\right]e(e^2-p^2)\chi(e,p)$$

$$\bar{Q} = \frac{\nu^2}{2} + \frac{(\xi-\xi_*)^2}{2(1-\gamma^2)} + \frac{5}{2}(3e^2+p^2)\xi^2 \qquad \xi \equiv -\nabla^2\zeta|_{\vec{r}=0}/\sigma_2$$

$$f_{\rm PBH}(M)d\ln M = \frac{M n_{\rm PBH}(M)}{\rho_{\rm DM}}d\ln M$$

$$n_{\rm PBH}(M) = \left(\int \mathcal{N}_{\rm pk}(\nu(M,e),\xi,e,p)|J|^{-1}d\xi dedp\right)/\sigma_0$$

Following C.M. Yoo, T. Harada, J. Garriga, K. Kohri. Arxiv: 1805.03946

We can rewrite the high of the peak in terms of the PBH mass using the Jacobian of the transformation $|J|(M,e) = \partial\mu/\partial\ln M$

But, we need to know the mass spectrum in terms of (e,p)...

PBH mass function including non-spherical effects

In this work, we don't compute numerical the PBH mass for non-spherical configuration, rather we follow existing results

In spherical symmetry, we know that the PBH mass will follow a scaling law (critical collapse)

Existing analytical and numerical studies indicate that, even in the presence of non-sphericities, black hole mass in the critical regime continues to follow a scaling law.
(collapse of non-spherical perfect fluids in asymptotically flat spacetime)

J. Celestino, T.W. Baumgarte. Arxiv: 1805.10442
T.W. Baumgarte, P.J. Montero. Arxiv:1509.08730

Perturbative analysis->non-spherical modes decay when 0.11<w<0.49.
C. Gundlach, ArXiv:gr-qc/9906124

$$M \sim (\mu - \mu_c(e))^\gamma$$

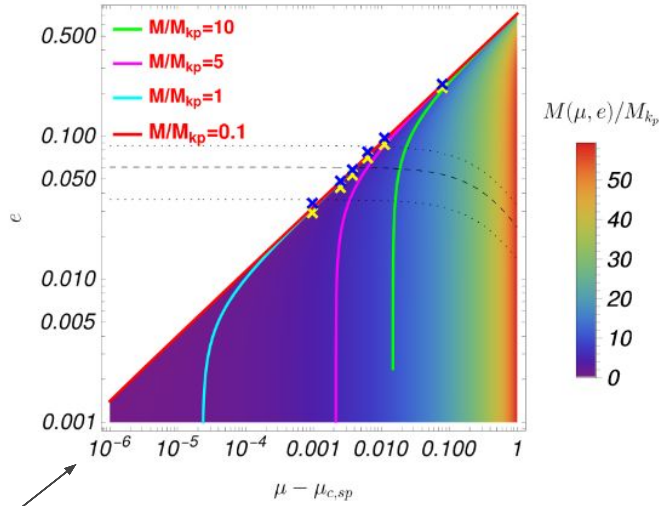

The mass now depends also on (e)

PBH mass function including non-spherical effects

$$n_{\rm PBH}(M) = \int de dp \sqrt{\frac{3}{\mathcal{A}_\zeta}} \left(\frac{5}{2\pi}\right)^{5/2} \nu(M,e)^8 W(e,p)$$
$$\times \exp\left\{-\frac{\nu(M,e)^2}{2}(1+15e^2+5p^2)\right\}|J|^{-1}(M,e)$$
$$|J|(M,e) \equiv \left|\frac{\partial \ln M}{\partial \mu}\right|$$
$$= \left|\frac{3(1+w)}{1+3w}\left(\frac{d\bar{\zeta}_{sp}(r_m;\mu)}{d\mu}\right)_{\mu=\mu(M,e)} + \frac{\gamma}{\mu(M,e)-\mu_c(e)}\right|$$

$$f_{\rm PBH}(M) d\ln M = \frac{M n_{\rm PBH}(M)}{\rho_{\rm DM}} d\ln M$$

"LET ME SIMPLIFY"

$$h_1(\nu,e) = -\frac{e}{125\nu^5}\left[\sqrt{10\pi}\left(25e^2\left(9e^2-1\right)\nu^4+\left(5-30e^2\right)\nu^2-9\right)\mathrm{erf}\left(\sqrt{\frac{5}{2}}e\nu\right)+10e\,\nu\,\exp\left\{-\frac{5}{2}e^2\nu^2\right\}\left(5\left(9e^2-1\right)\nu^2+9\right)\right]$$

$$h_2(\nu,e) = -\frac{e}{250\nu^6}\left[\sqrt{10\pi}\nu\left(25e^2\left(9e^2-1\right)\nu^4+\left(5-30e^2\right)\nu^2-9\right)\mathrm{erf}\left(\sqrt{\frac{5}{2}}(1-3e)\nu\right)\right.$$
$$+\sqrt{10\pi}\nu\left(25e^2\left(9e^2-1\right)\nu^4+\left(5-30e^2\right)\nu^2-9\right)\mathrm{erf}\left(\sqrt{\frac{5}{2}}e\nu\right)$$
$$-2\exp\left\{-\frac{5}{2}\left(9e^2+1\right)\nu^2\right\}\left(\exp\{15e\nu^2\}\left(25e^2(3e+1)\nu^4+5\left(32e^2-21e-1\right)\nu^2+16\right)+\right.$$
$$\left.\left.+\exp\left\{\frac{5}{2}\left(8e^2+1\right)\nu^2\right\}\left(-225e^3\nu^4+160e^2\nu^2+5e\left(5\nu^2-9\right)\nu^2-16\right)\right)\right].$$

$$n_{\rm PBH}(M) = \int_{e=0}^{e=1/4} g(M,e) h_1(\nu(M,e),e) de$$
$$+ \int_{e=1/4}^{e=1/2} g(M,e) h_2(\nu(M,e),e) de$$
$$g(M,e) = \sqrt{\frac{3}{\mathcal{A}_\zeta}}\left(\frac{5}{2\pi}\right)^{5/2}$$
$$\times \exp\left\{-\frac{\nu(M,e)^2}{2}(1+15e^2)\right\}\nu(M,e)^8 |J|(M,e)$$

PBH mass function including non-spherical effects (FINAL RESULT)

Conclusion: for the case tested, non-spherical effects play a very small role

The critical regime plays a crucial role

large value of the amplitude can contribute to the abundance of the small mass PBH with (e) very close to ec(μ).

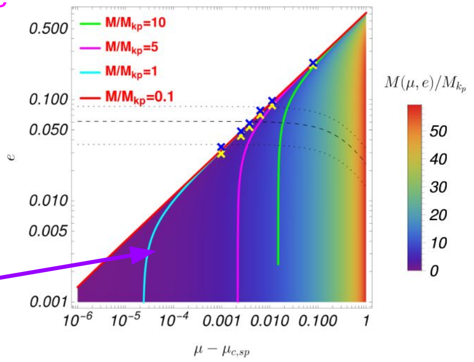

The mass function will be dominated by fluctuations that are very close to its critical μc(e)

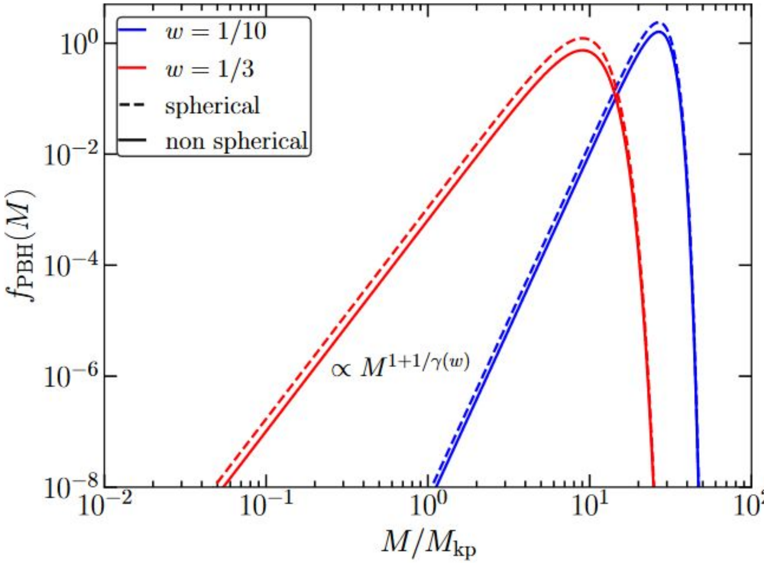

Conclusions

- We find that the critical (ec,pc) follows a superellipse curve with a similar exponent for both equations of state. Universality?

- In the range of amplitudes considered, we find a decaying power law behaviour for the ellipticity (e) with p=0.

- Non-spherical effects are crucial, with fluctuations in the critical regime, avoiding fluctuations to collapse and forming a black hole in comparison with the spherical case.

- For the case tested, we find that non-spherical effects has a very small effect on the PBH mass function